Sentinel lymph node detection *ex vivo* using ultrasound-modulated optical tomography

Chulhong Kim, Kwang Hyun Song, and Lihong V. Wang
Washington University in Saint Louis
Optical Imaging Laboratory
Department of Biomedical Engineering
Campus Box 1097
One Brookings Drive
Saint Louis, Missouri 63130-4899
E-mail: lhwang@biomed.wustl.edu

Abstract. We apply ultrasound-modulated optical tomography (UOT) to image *ex-vivo* methylene-blue-dyed sentinel lymph nodes embedded in 3.2-cm-thick chicken breast tissues. The UOT system is implemented for the first time using ring-shaped light illumination, intense acoustic bursts, and charge-coupled device (CCD) camera-based speckle contrast detection. Since the system is noninvasive, nonionizing, portable, relatively cost effective, and easy to combine with photoacoustic imaging and single element ultrasonic pulse-echo imaging, UOT can potentially be a good imaging modality for the detection of sentinel lymph nodes in breast cancer staging *in vivo*. © *2008 Society of Photo-Optical Instrumentation Engineers.* [DOI: 10.1117/1.2907791]

Keywords: ultrasound-modulated optical tomography; sentinel lymph node biopsy; breast cancer; axillary lymph node dissection; speckle contrast; acoustic bursts.

Paper 07492LR received Jan. 3, 2008; revised manuscript received Feb. 18, 2008; accepted for publication Feb. 18, 2008; published online Apr. 21, 2008.

For the majority of invasive breast cancers, the surgical removal of primary breast tumor and levels I and II axillary lymph node dissections (ALND) are widely performed.[1] However, the common side effects after ALND include upper-extremity lymphedema, arm numbness, impaired shoulder mobility, arm weakness, and infections in the breast, chest, or arm.[2] Therefore, as a less invasive alternative to ALND, sentinel lymph node biopsy (SLNB), that is, biopsy of the first lymph node receiving drainage from a cancer-containing area of the breast, has become increasingly important in breast cancer treatment.[3] By reducing the number of ALND, the risk of side effects can be alleviated.[3] Although SLNB with methylene blue dye and radioactive tracers has an identification rate of 90 to 95%, the widely used detection of gamma radiation using a gamma camera is ionizing and intraoperative.[3,4] Since ultrasound-modulated optical tomography[5] (UOT) is able to image optical contrast with high ultrasonic spatial resolution, as is photoacoustic imaging,[6] nonionizing UOT has the potential to detect methylene-blue-dyed SLNs noninvasively. In addition, thanks to the use of a relatively cost effective and small continuous wave (cw) diode laser, the UOT can potentially be clinically more attractive for the detection of SLNs than photoacoustic imaging, which usually requires a bulky and relatively expensive pulsed laser.

The principle of UOT is based on the phase modulation of multiply scattered light inside biological tissues during focused ultrasonic insonification. The phase modulation mainly comes from both ultrasound-induced particle displacement and changes in refractive index. By measuring the level of modulation at each scanned ultrasonic focal point, images represent the optical properties of the tissue. The mechanisms of UOT have been studied theoretically by Leutz and Maret,[7] Wang,[8] and Sakadžić and Wang.[9] Experimentally, a number of detection methods have been pioneered to detect weakly modulated signals efficiently.[10–12]

In this work, for the first time to our knowledge, we report the use of UOT to detect *ex-vivo* methylene-blue-dyed SLNs buried in chicken breast tissues. In addition, UOT is compared with photoacoustic imaging and single-element ultrasonic pulse-echo imaging. The UOT system is implemented, also for the first time, with ring-shaped light illumination, intense acoustic bursts, and CCD camera-based speckle contrast detection.[13] Since the light source (a cw diode laser), ultrasonic transducer, and light detector [a charge-coupled device (CCD) camera] are mounted on a single frame, the UOT system is portable and relatively cost effective. Moreover, three imaging techniques such as UOT, photoacoustic imaging, and single-element ultrasound pulse-echo imaging can be potentially merged into a single system.

The experimental schematic is shown in Fig. 1, which is analogous to the setup in Ref. 6. The ring-shaped light illumination is formed sequentially by a plano-concave lens, a spherical conical lens, and an optical condenser. This illumination has an advantage over previous illumination

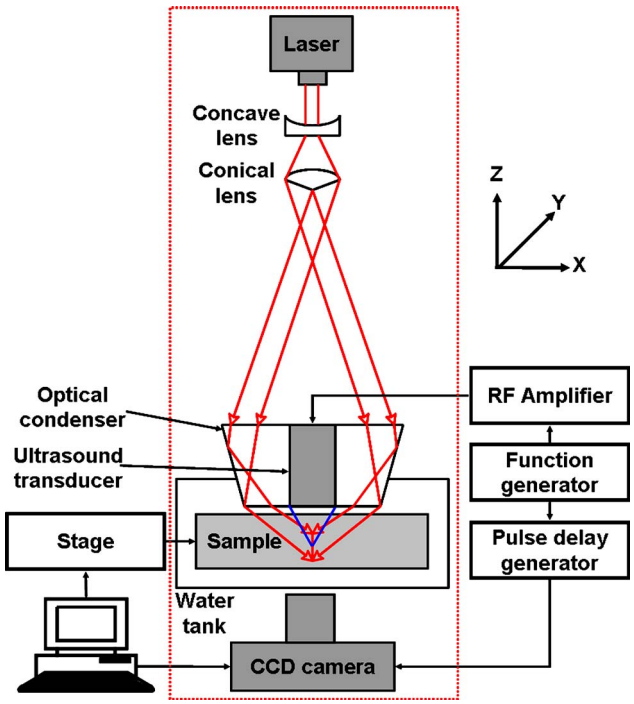

Fig. 1 Schematic of the ring-shaped light illumination UOT system.

Address all correspondence to Lihong Wang, Biomedical Engineering, Washington University in St. Louis, One Brookings Drive, Campus Box 1097-Campus Box 1097, St. Louis, Missouri 63130 United States of America; Tel: (314) 935-6152; Fax: (314) 935-7448; E-mail: lhwang@biomed.wustl.edu

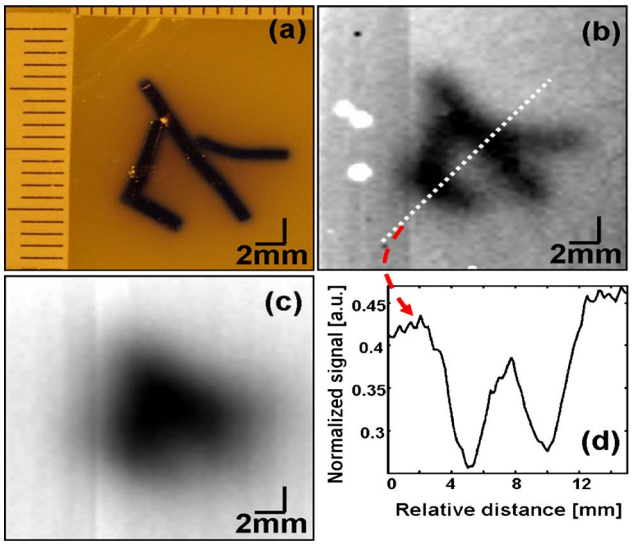

Fig. 2 Cross-sectional UOT images of an optically absorptive patterned object. (a) Photograph of the target. (b) UOT image based on change in speckle contrast. (c) Image based on light intensity. (d) 1-D profile along the cut in.

geometries:[5,10,12,13] it can reduce the shadow effect of light along the light propagation direction, since the light is more evenly distributed. Because of shadows, the previous transmission-mode technique with cw ultrasound required image processing to achieve a good quality cross sectional image. By contrast, the ring geometry can provide a cross sectional image with less shadow if the imaging plane is parallel to the plane of the doughnut shape of the illumination. To make the system compact and relatively inexpensive, we utilized a small diode laser (Melles Griot, 56ICS153/HS; 657-nm wavelength; $9\times6\times13$ cm along the x, y, and z axes) mounted on the same post as the optics. The peak absorption of methylene blue occurs around the laser wavelength. An average laser power of $\sim$24.5 mW/cm^2 was delivered to the tissue. A narrowband, high-power, focused ultrasound transducer (Panametrics, A320S-SU; 7.5-MHz central frequency; 12.7-mm active aperture; 19.7-mm focal length; 50% bandwidth) was placed into the middle of the optical condenser. The transducer was partially immersed in water inside a tank that had an opening at the bottom sealed with a thin, disposable, clear membrane. The ultrasonic focus was aligned with the line focus of light in water. A peak pressure of up to 3.2 MPa was applied to the ultrasonic focal point, so the mechanical index at this frequency was less than 1.2, within the typical safety limit. The sample was located inside the water tank and connected to an automatic scanning stage controlled by a computer for raster scanning. A CCD camera (Basler, A312f; 12 bit, 640×480 pixels) was positioned underneath the water tank, and the main axis of the camera was aligned with the ultrasound propagation axis. The components in the dotted box in Fig. 1 were all built on a single frame. The CCD camera captured speckle patterns formed by light transmitted through the sample. A function generator (Agilent, 33250A) produced acoustic bursts, which were amplified by an RF amplifier (Amplifier Research, 75A250). Simultaneously, the CCD camera was triggered twice during each burst by a pulse-delay generator (Stanford

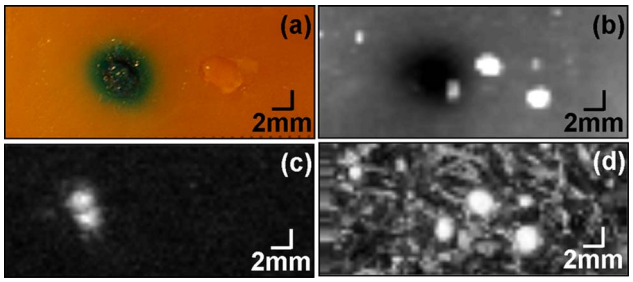

Fig. 3 *Ex-vivo* cross sectional images of two sentinel lymph nodes in 1.2-cm-thick chicken breast tissue. (a) Photograph of two nodes; the left node is dyed with methylene blue and the right one is not. (b) UOT image. (c) Photoacoustic image. (d) Single-element ultrasound pulse-echo image.

Research, DG535) synchronized with the function generator. One CCD frame synchronized with the burst initiation was captured with ultrasound; subsequently, another one was captured without ultrasound. We used a low 0.83-Hz ultrasound burst repetition rate to prevent damage to the transducer. The exposure time of the CCD camera was set to 1 or 2 ms, equivalent to the duration of an ultrasonic burst. The laser speckle contrast, defined as $\sigma_I/\langle I\rangle$, where σ_I is the standard deviation of intensity in the speckle pattern and $\langle I\rangle$ is the mean of the intensity, was measured with and without ultrasound modulation. The UOT signal was defined as the change in speckle contrast between the ultrasound on and off conditions. We averaged two or three pairs of on-off measurements.

To investigate the potential for cross sectional imaging using this UOT system, we scanned a 1-cm-thick tissue phantom that contained an optically absorptive patterned object. The phantom was made of 10% gelatin by weight and 1% intralipid by volume, and its reduced scattering coefficient was $\sim$9 cm^{-1}. The thickness of the patterned shape along the ultrasound propagation direction was about 1 mm. An acoustic peak pressure of 1.6 MPa was applied to the sample. The patterned shape is clearly resolvable in Fig. 2(b) and matches well with the photograph in Fig. 2(a), whereas the unmodulated light intensity based image in Fig. 2(c) cannot resolve the shape. Figure 2(d) shows a 1-D profile taken from the image in Fig. 2(b). The spatial resolution, defined as the one-way distance across the 25 and 75% points between the maximum and minimum of the edge spread function, is 870 ± 59 μm (standard error). The SNR, defined as the mean of the change in speckle contrast between ultrasound on and off divided by its root-mean-square standard deviations, is 199 ± 13 (standard error).

To show the feasibility of imaging SLNs containing methylene blue dye, we scanned 1.2-cm-thick chicken breast tissues containing two excised lymph nodes. The animal handling was performed in compliance with guidelines on the care and use of laboratory animals at Washington University in Saint Louis. First, an intradermal injection of 0.12 ml of 1% methylene blue dye (10 mg/mL, American Regent, INC) was performed on the right forepaw pad of an adult male Sprague Dawley rat weighing 300 g. About 15 min after administration of the methylene blue dye, the animal was euthanized with an overdose of pentobarbital. One methylene-blue-dyed lymph node was excised from the right side of the animal and another one from the left side (without any dye).

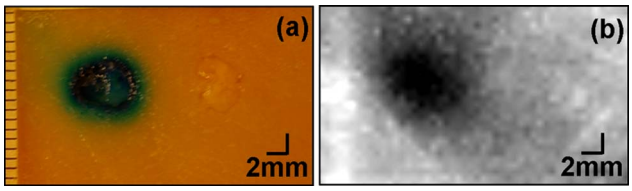

Fig. 4 *Ex-vivo* cross sectional images of two sentinel lymph nodes in 3.2-cm thick chicken breast tissue. (a) Photograph of two nodes; the left node is dyed with methylene blue and the right one is not. (b) UOT image.

The two excised nodes ($3 \times 5 \times 2$ mm along the x, y, and z axes) were buried between two chicken breast slices. Only the methylene-blue-dyed node is clearly seen with an image contrast of 57% in Fig. 3(b), and matches well with the photograph in Fig. 3(a). To confirm the UOT image, we scanned the sample using a photoacoustic imaging system,[6] which had a similar configuration to the UOT system. A 5-MHz ultrasound transducer and a 770-nm laser beam were used. Even though the light wavelength was not optimal for methylene blue dye absorption, which peaks at 670 nm, only the dyed node is clearly seen in Fig. 3(c). In addition, air bubbles in the interface between the two chicken slices were also imaged in the UOT image [Fig. 3(b)]. To confirm the existence of air bubbles, single-element ultrasound pulse-echo imaging was executed using the photoacoustic imaging system. The distribution of air bubbles in the UOT image [Fig. 3(b)] matches well with the one in the pulse-echo image [Fig. 3(d)].

To examine the feasibility of this technology for clinical application, the total thickness of chicken tissue was increased up to 3.2 cm, and the experiment was repeated. Only the methylene-blue-dyed node is clearly seen with an image contrast of 57% in Fig. 4(b), and the image matches well with the photograph in Fig. 4(a).

In conclusion, this research produces images of *ex-vivo* methylene-blue-dyed sentinel lymph nodes using ultrasound-modulated optical tomography in biological tissues up to 3.2 cm thick. The UOT system with the ring-shaped light illumination has several advantages. 1. It is nonionizing and noninvasive, unlike ionizing and intraoperative gamma-radiation-based detection. 2. It is portable and cheaper than photoacoustic imaging. 3. It is possible to combine three imaging techniques such as UOT, photoacoustic imaging, and single-element ultrasound pulse-echo imaging into one single imaging system. On the basis of these features and the initial experimental study, this technique can potentially be extended to image SLNs containing methylene blue dye in humans *in vivo*.

Acknowledgments

This research was supported by NIH grant numbers R33 CA 094267, R01 NS46214, and R01 CA106728.

References

1. "Early stage breast cancer," *Consens Statement* 8:1 (1990).
2. K. K. Swenson, M. J. Nissen, C. Ceronsky, L. Swenson, M. W. Lee, and T. M. Tuttle, "Comparison of side effects between sentinel lymph node and axillary lymph node dissection for breast cancer," *Ann. Surg. Oncol.* **9**(8), 745–753 (2002).
3. K. M. McMaster, T. M. Tuttle et al., "Sentinel lymph node biopsy for breast cancer: a suitable alternative to routine axillary dissection in multi-institutional practice when optimal technique is used," *J. Clin. Oncol.* **18**(13), 2560–2566 (2000).
4. O. A. Ung, "Australian experience and trials in sentinel lymph node biopsy: the RACS SNAC trial," *Asian J. Surg.* **27**(24), 284–290 (2004).
5. L. V. Wang, S. L. Jacques, and X. Zhao, "Continuous-wave ultrasonic modulation of scattered laser light to image objects in turbid media," *Opt. Lett.* **20**(6), 629–631 (1995).
6. K. H. Song and L. V. Wang, "Deep reflection-mode photoacoustic imaging of biological tissue," *J. Biomed. Opt.* **12**(6), 060503-(1-3) (2007).
7. W. Leutz and G. Maret, "Ultrasonic modulation of multiply scattered light," *Physica B* **204**(1), 14–19 (1995).
8. L. V. Wang, "Mechanisms of ultrasonic modulation of multiply scattered coherent light: an analytic model," *Phys. Rev. Lett.* **87**(4), 043093 (2001).
9. S. Sakadžic and L. V. Wang, "Correlation transfer and diffusion of ultrasound-modulated multiply scattered light," *Phys. Rev. Lett.* **96**(16), 163902 (2006).
10. S. Leveque, A. C. Boccara, M. Lebec, and H. Saint-Jalmes, "Ultrasonic tagging of photon paths in scattering media: parallel speckle modulation processing," *Opt. Lett.* **24**(3), 181–183 (1999).
11. S. Sakadžić and L. V. Wang, "High-resolution ultrasound-modulated optical tomography in biological tissues," *Opt. Lett.* **29**(23), 2770–2272 (2004).
12. T. W. Murray, L. Sui, G. Maguluri, R. A. Roy, A. Nieva, F. Blonigen, and C. A. DiMarzio, "Detection of ultrasound-modulated photons in diffuse media using the photorefractive effect," *Opt. Lett.* **29**(21), 2509–2511 (2004).
13. C. Kim, R. J. Zemp, and L. V. Wang, "Intense acoustic bursts as a signal-enhancement mechanism in ultrasound-modulated optical tomography," *Opt. Lett.* **31**(16), 2423–2425 (2006).